Chemical speciation of copper(II) diaminediamide derivative of pentacycloundecane—a potential anti-inflammatory agent

Sebusi Odisitse,[a] Graham E. Jackson,[a] Thavendran Govender,[b] Hendrik G. Kruger[b] and Amith Singh[b]

Received 12th October 2006, Accepted 26th January 2007
First published as an Advance Article on the web 8th February 2007
DOI: 10.1039/b614878f

Formation constants of copper(II), zinc(II) and calcium(II) with 3,5-diaminodiamido-4-oxahexacyclododecane (cageL) has been studied by glass electrode potentiometry at 25 °C and an ionic strength of 0.15 mol dm^{-3}. Copper(II) forms more stable complexes with cageL than zinc(II) and calcium(II). Metal ion complexation promotes deprotonation and coordination of the amide nitrogens resulting in overall tetragonal coordination of Cu^{2+} suggested by the UV-visible electronic spectra. Speciation calculations using a blood plasma model suggest that zinc(II) and calcium(II) are good competitors of copper(II) *in vivo.* Bio-distribution experiments using ^{64}Cu-labelled Cu(II)-cageL show that about 50% dose of the complex is retained in the body after 24 h.

Introduction

Rheumatoid arthritis (RA) is a debilitating disease affecting some 5% of the Western World.[1] There is no cure, however, the symptoms and progression of the disease can be controlled using immunosuppressive and anti-inflammatory drugs.[2,3] Copper complexes were observed to be effective in the treatment of RA and other degenerative connective tissue diseases as early as 1941.[4,5] Indeed, the copper bangle has been used for centuries.[7] More recently, we and others have shown that copper complexes are able to alleviate the inflammation associated with RA.[7–13] Serum copper levels are elevated during RA and it has been postulated that endogenous copper might have a protective function in chronic inflammatory conditions.[4–7] With this in mind, we have embarked on a programme of ligand design with the objective of producing a ligand which will complex copper and increase its bioavailability and at the same time not disrupt the homeostasis of other endogenous metal ions. To this end, the ligand has to be a strong chelator of copper, although it should not be so strong that the complex is excreted intact before the copper can exert its therapeutic potential. The complex should also be primarily a nitrogen donor ligand so that the selectivity for copper is increased. The concentrations of calcium(II) and zinc(II) in blood plasma are far higher than that of copper(II) and the ligand would have to overcome this concentration differential in order to bind to copper(II) *in vivo.* The complex should also be kinetically labile to be able to release the copper at the active site and should be lipophilic in order to be absorbed dermally.

The above criteria led to the design of the polyamine ligands 3,6,9,12-tetra-azatetradecanedioic acid (L^6) and 3,6,9-triazatetradecanedioic acid (L^7).[8,14] In animal tests, these ligands proved to be powerful chelators of copper, so much so that they were rapidly excreted, unchanged, in urine. Although these complexes were formally neutral, being dicarboxylic acids, they were still hydrophilic and hence were cleared from the body *via* the kidneys. In order to improve the lipophilicity of the complex, mixed amino/amido ligands were designed in which coordination to the metal would lead to deprotonation of the amide nitrogen and a neutral complex.[10] Partition coefficient measurements showed that these complexes were indeed more lipophilic with 5% of the complex going into the organic layer. In order to further improve the lipophilicity, the pentacyclo-undecane derived ligand 3,5-diaminodiamido-4-oxahexacyclo[5.4.1.$0^{2,6}$.$0^{3,10}$.$0^{5,9}$.$0^{8,11}$]dodecane (cageL) shown in Fig. 1 was designed. This ligand has the amino/amido coordinating structure used before but now attached to a pentacyclo-undecane derivative.

The chemistry of pentacyclo-undecane cage derivatives has been extensively studied.[15–17] A number of amino cage compounds have promising potential medicinal and pharmaceutical activities.[18–23] The advantages of incorporating a rigid cage structure into bioactive compounds has been extensively reported.[24–30] Due to the large lipophilic nature of the cage moiety it was able to cross various membranes quite efficiently. An added advantage, is that the rigidity of the cage should increase the stability of the metal complex by forcing the ligand into an ideal conformation for complexation.

Results and discussion

Ligand synthesis

The diaminodiamido cage ligand was synthesized from pentacyclo-undecane dione as illustrated in Scheme 1.

The dione is photocyclized from the Diels–Alder adduct between *p*-benzoquinone and cyclopentadiene.[31] Treatment of the dione with allylmagnesium bromide produced the *endo–endo* diol **2**.[32–33] The subsequent reactions to synthesize the intermediates up to the acid chloride **5** have been described previously.[34–36] The novel ester **6** was obtained through reaction of the acid chloride with excess ethanol. The required diaminodiamido cage ligand **7** was obtained by treatment of the ester **6** with ethylenediamine (see Scheme 2).

[a]*Department of Chemistry, University of Cape Town, Private Bag Rondebosch, 7701, South Africa*
[b]*School of Chemistry, University of KwaZulu-Natal, Durban, 4041, South Africa. E-mail: jackson@science.uct.ac.za*

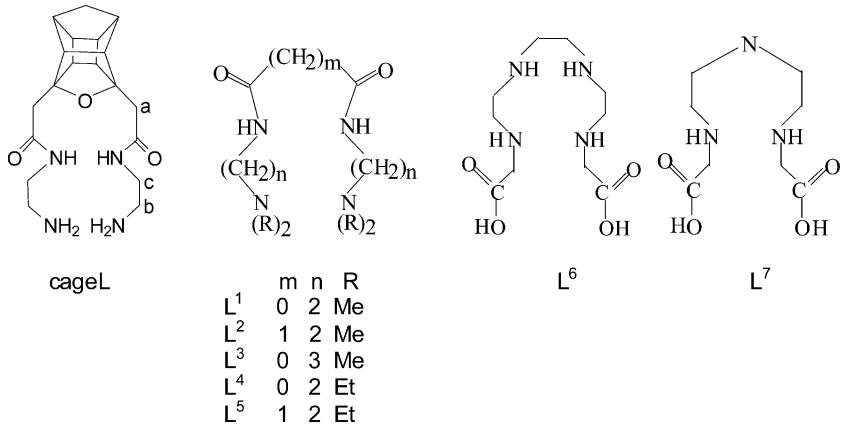

Fig. 1 Schematic diagrams of cageL and related ligands.

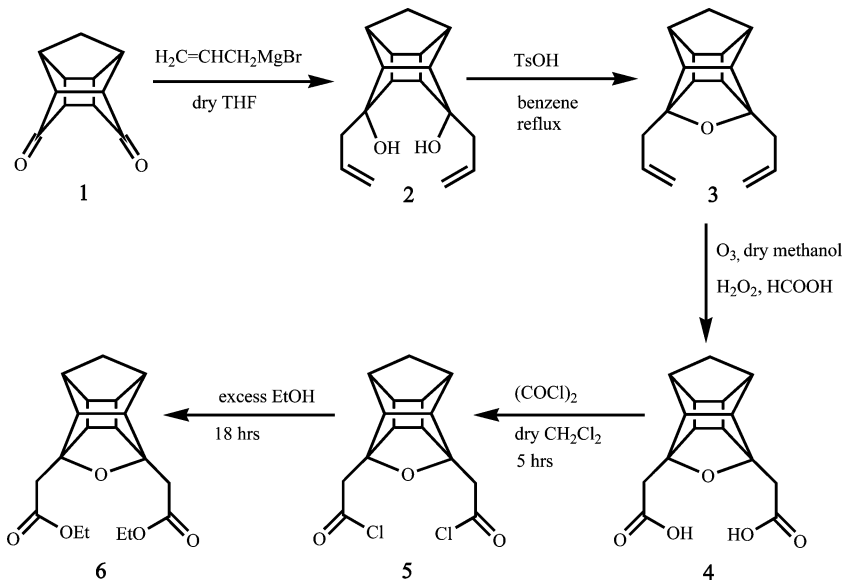

Scheme 1

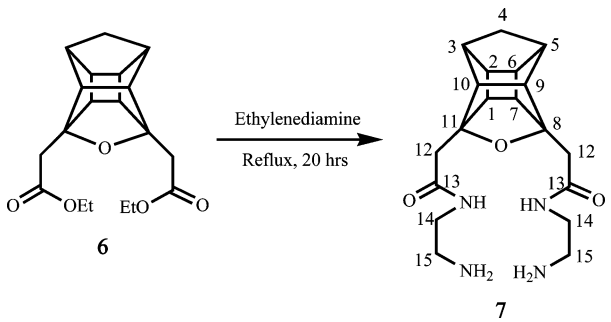

Scheme 2

The ^{13}C NMR spectrum of the diaminodiamido ligand **7** shows the amide carbonyls at 170.05 ppm, quaternary carbons at 93.6 ppm and methylene carbons C-12, C-14 and C-15 at 39.3 ppm, 41.6 ppm and 41.0 ppm, respectively. The "cage" carbons are reported in the Experimental section. The ^{1}H NMR spectrum shows two doublets (doublet of doublets) that are due to protons H-4a (1.40 ppm) and H-4s (1.75 ppm) coupling with protons at the two non-equivalent sides of the cage. The peak at 7.19 ppm shows the presence of the amide N–H proton. The multiplet at 3.13 ppm can be attributed to methylene protons H-15. The relative flat proton signal at 1.9 ppm was assigned to the amino protons.

Potentiometry

The protonation constants for the two terminal amine groups of cageL are given in Table 1. The first protonation constant is lower than that of methylamine because of the electronic withdrawal effect of the amide. Similarly, pK_{a1} is 1.23 log units greater than pK_{a2} because of the electrostatic repulsion of the first proton.

We have used the complex formation (Z_M-bar)[37,38] (eqn (1)) and deprotonation functions (Q-bar)[38,39] (eqn (2)) as criteria in speciation model selection where the former measures the number of ligands bound per metal ion while the latter indicates the number of protons released upon metal ion complexation. The two functions are derived from the free and total concentrations of the participating components as well as the evaluated protonation constants. The classical Z_M-bar function is strictly only defined for simple mononuclear complex formation. However, deviations from ideal behaviour are indicative of the different speciation

Table 1 Logarithms of overall stability constant, β_{pqr}, of copper(II), zinc(II) and calcium(II) complexes of cageL at 25 °C and ionic strength 0.15 mol dm^{-3} NaCl. R^H is the Hamilton *R*-factor, R_{lim} is the minimum *R*-factor based on the estimated errors in the analytical data. The standard deviation in the log β is given in parentheses. The general formula of the complex $M_pL_qH_r$ is denoted by the coefficients *pqr*

Metal	*p*	*q*	*r*	Log β_{pqr}	R^H	R_{lim}
H^+	0	1	1	9.52(1)	0.01	0.02
	0	1	2	17.81(2)		
Cu(II)	1	1	1	15.50(3)	0.02	0.02
	1	1	0	9.96(2)		
	1	1	−1	2.71(3)		
	1	1	−2	−7.05(4)		
Zn(II)	1	1	1	13.81(4)	0.01	0.03
	1	1	0	5.55(3)		
	1	1	−1	−2.93(4)		
	1	1	−2	−11.74(3)		
Ca(II)	1	1	1	13.19(3)	0.01	0.02
	1	1	0	3.80(3)		
	1	1	−1	−7.57(6)		

occurring. Thus, if the curves at different metal : ligand ratios are not superimposable, protonated or polynuclear species formation is indicated, while if the curves fan back hydroxyl species formation is indicated.

Z_M-bar and *Q*-bar are defined by:

$$Z_M\text{-bar} = (T_L - [L])/T_M \quad (1)$$

$$Q\text{-bar} = (T_H^* - T_H)/T_M \quad (2)$$

Where T_L, T_M and T_H refer to the total ligand, metal and proton concentration, respectively, [L] is the free ligand concentration and T^*_H is the calculated total concentration of protons that would be necessary to obtain the same pH if no complexation took place.

Fig. 2 shows the Z_M-bar function for the Cu(II)–cageL system plotted against pL (−log[L]). These curves at different metal-to-ligand ratios were not superimposable, indicating the presence of polynuclear or protonated species. At low pL or high pH the curves fanned back indicating the formation of hydroxy species. The same speciation is shown by the *Q*-bar curves. Again these curves are not superimposable and cut the *n*-bar curve around pH 6.0. Since the *n*-bar curve is a plot of the number of protons that would be bound to the ligand at a particular pH in the absence of the metal ion, if the *Q*-bar is greater than *n*-bar, it means that more protons have been lost from the ligand than the ligand had to lose. That is an hydroxy species has formed.

The potentiometric data were analysed using the ESTA suite of computer programs[39] which yielded the results given in Table 1. The low standard deviation in the log β's, the low Hamilton factors and the agreement between the observed and calculated data lend confidence to the results. In fact $R^H \approx R_{lim}$, means that it is not statistically possible to improve the model. It is interesting to note that the stability of the Cu(II)–cageL complexes is greater than its non-cage analogue. It was anticipated that this would be the case because in cageL, the ligand is pre-formed in the correct conformation for metal-ion coordination. A species distribution diagram, calculated using the data in Table 1 is shown in Fig. 3. From this we see that complexation commences at about pH 3 when the protonated MLH species is formed. At pH 6, the ML species predominates while at pH 8.5 most of the copper is in the MLH_{-1} species.

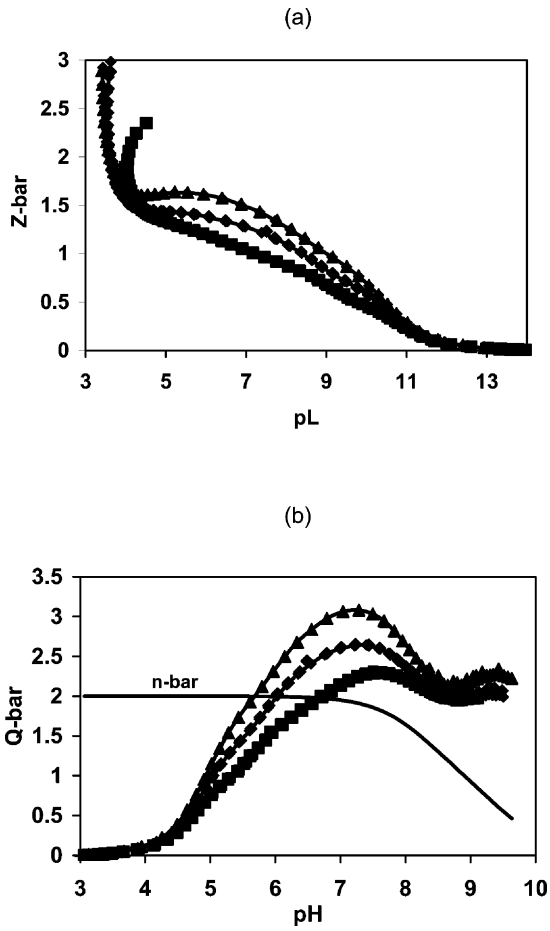

Fig. 2 Experimental and theoretical (a) *Z*-bar and (b) *Q*-bar curves for the Cu(II)-cageL system at 25 °C and an ionic strength of 0.15 M (Cl^-). M : L ratios 1 : 2 (■), 1 : 3 (◆), 1 : 4 (▲) are displayed. The theoretical line was calculated using the model given in Table 1.

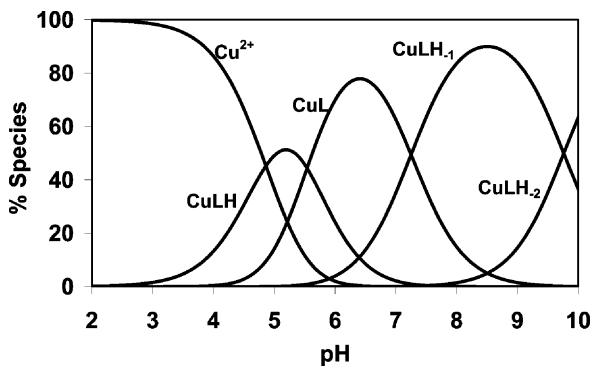

Fig. 3 Speciation distribution curves for a Cu(II)–cageL solution (with M : L of 1 : 1 and [cageL] = 0.0034 mol dm^{-3}) plotted as a function of pH.

Zn(II) and Ca(II) were also found to form complexes with cageL albeit less stable complexes (Table 1). The order of stability Cu(II) > Zn(II) > Ca(II) is as expected.[40] These two metal ions were studied because they are potential competitors of Cu(II) *in vivo*. Even though they are weaker chelators than Cu(II), their *in vivo* concentration is far higher and so they could potentially compete.

From the potentiometric data it is not possible to tell the structure of the different complexes formed. However, by comparison

Table 2 Wavelengths corresponding to maximum absorption coefficients of the various Cu(II) species formed in solution with cageL

λ_{max}/nm, ε/dm^{3}mol^{-1} cm^{-1}			
M	MLH	ML	MLH_{-1}
790	720	660	590
13.2	27.4	44.2	95.5

with known systems, it is possible to make some inference as to the site of coordination. Ligands L^1 and L^2 in Fig. 1 are similar to cageL but do not have the cage moiety.

Solution structures

During the pH titration of the Cu(II)–cageL system, the colour of the solution changed from blue to blue–violet. Electronic spectra were recorded for this system as a function of pH. A single broad absorption band was observed which envelopes the expected spin allowed $^2A_{1g} \leftarrow {}^2B_{1g}$, $^2B_{2g} \leftarrow {}^2B_{1g}$ and $^2E_g \leftarrow {}^2B_{1g}$ transitions of a tetragonally distorted copper complex.[41] Analysis of the data yielded the λ_{max} and molar extinction coefficients listed in Table 2. Electronic spectra are useful because the energy of the transition is influenced by the coordination sphere of the metal ion. Thus λ_{max} affords a measure of the solution structure of the complex.

Computer optimized structures for the MLH species are shown in Fig. 4. The log K for the equilibrium M + LH $\leftrightarrow$ MLH is 6.0. Given the basicity of the amine, this value is too high for monodentate coordination (*cf.* methylamine, $pK_a = 10.6$; $\beta_{110} = 4.1$).[42]

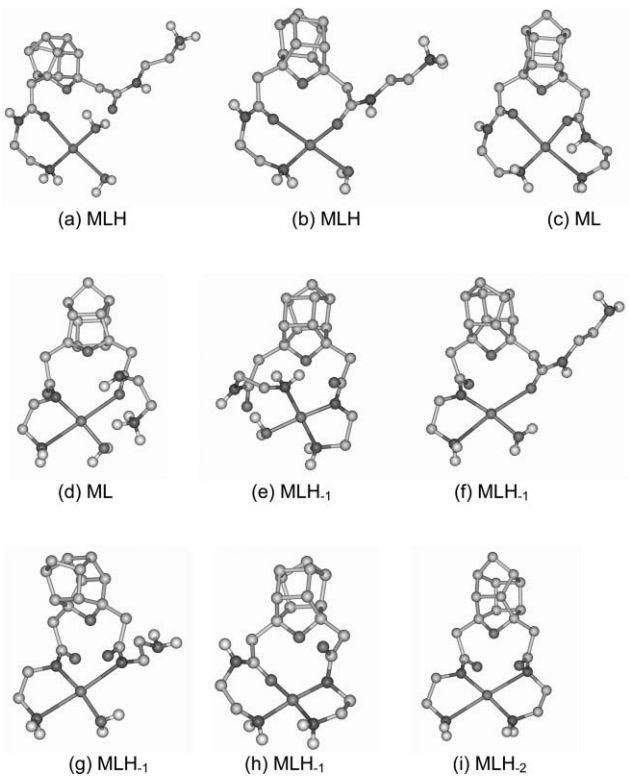

Fig. 4 Optimised structures for the different possible isomers of Cu(II)–cageL, For clarity axial waters and hydrogen atoms bonded to carbon atoms have been omitted.

Structure 4(a) has the metal bidentately coordinated to one terminal amine and a carbonyl oxygen. The other terminal amine is still protonated giving the correct stoichiometry. Billo[43] and subsequently Sigel and Martin[44] have proposed a simple empirical method of estimating the electronic energy of a proposed configuration. If one amine is coordinated to the copper a λ_{max} of 743 nm is expected and with two amines a λ_{max} of 661 nm is expected. The λ_{max} of the MLH species is 720 nm which is much closer to the value for single amine coordination. Since we believe the ligand is bidentate the carbonyl oxygen must be coordinated. This would not change λ_{max}. Further support for this conclusion comes from the demonstration that with copper(II)–glycinamide (pK_a 7.93)[42] and β-alaninamide (pK_a 9.19)[42] the metal coordinates through the amine and the carboxyl group with log β of 5.3 and 5.1, respectively.[42] These values are very similar to the log K of 6.0 for our system where the $pK_1 = 9.52$. It is possible for both carbonyl groups to be coordinated as depicted in Fig 4(b). The UV-visible spectrum of this structure would be similar to that of structure 4(a) as would their formation constants. Hence we cannot distinguish between these two structures.

Loss of a proton from the MLH species gives rise to the ML complex. If structure 4(b) is the correct structure for MLH then ML could form by coordination of the second terminal amine to give structure 4(c). Alternatively, one of the amides could deprotonate to give structure 4(d) where the second carbonyl may or may not be coordinated. The pK_a for this process (log β_{110} − log β_{111}) is 5.0. This can be compared to the same process occurring with glycinamide (pK_a 6.8) where it is known that coordination swaps from the amide oxygen to the amide nitrogen.[44] λ_{max} for the ML complex of cageL is 660 nm. Structure 4(c) and 4(d) have calculated λ_{max} values of 661 and 646 nm, respectively. Hence we conclude that the ML species has structure 4(c).

Desseyn *et al.*[45] have proposed a structure in which only the two amines are coordinated to the metal. This structure also has a calculated λ_{max} of 661 nm. We believe, however, that the size of the chelate ring argues against this structure. Comparing 1,2-ethylenediamine ($pK_1 = 9.89$; $pK_2 = 7.08$),[42] 1,3-propylenediamine ($pK_1 = 10.56$; $pK_2 = 8.76$)[42] and 1,4-butylenediamine ($pK_1 = 10.72$; $pK_2 = 9.44$),[42] which form 5,6 and 7 membered chelate rings, the copper binding constants are 10.5, 9.7 and 8.6, respectively.[42] The increasing basicity of the amines should increase the stability of the complex but this is countered by the decreased chelate effect. If only the two terminal amines of CageL were to coordinate there would be no chelate stabilisation. However, its log β_{110} is 9.96 while pK_1 is 9.52 and pK_2 is 8.289.

Structures 4(e)–4(h) are all possible for the MLH_{-1} species. From the λ_{max} value for this complex of 590 nm structure 4(f) can be eliminated. The other possible structures have calculated λ_{max} values between 573 and 584. Structure 4(e) has been proposed by Zuberbüler and Kaden[46] but we do not favour this structure because of the large chelate ring.

Structure 4(g) requires that both amides are deprotonated while the terminal amine remains protonated. The pK_a for the loss of a proton from ML to form MLH_{-1} is 7.2. This value is below pK_{a2} (8.3) but one may argue that electronic repulsion from the charged metal center would decrease the basicity of the amine. Also, this complex exists in the pH range 7–10. At this high pH, it is unlikely that the terminal amine would remain protonated while the amides deprotonated. If the amide were to coordinate

to the metal ion then it would be easy for the amine to coordinate giving the MLH_{-2} stoichiometry. Similarly structure 4(f), where the carbonyl oxygen is coordinated and the unprotonated amine is not, is unlikely. Hence we favour structure 4(h) for the MLH_{-1} species.

MLH_{-2} forms from the deprotonation of MLH_{-1} with a pK_a of 9.7. This proton could come from a coordinated water molecule or from the uncoordinated amide nitrogen. The hydrolysis constant of $[Cu(H_2O)_6]^{2+}$ is 7.87, but this is for an equatorially coordinated water molecule. Because of Jahn–Teller distortion, hydrolysis of axial water will be much lower (*i.e.* the pK_a would be much higher). Hence it is possible that the proton comes from water. However, we have shown that coordination of OH^- in the axial position causes a 20 nm red shift in λ_{max}. While we were unable to obtain the electronic spectrum of MLH_{-2}, spectra for related ligands L^1–L^5 all show a substantial blue shift.[9,10] Thus we propose that deprotonation of the amide occurs and the ligand rearranges to give structure 4(i). This structure is supported by several other studies[47] including the crystal structure of Ni–L^3.[48]

Nuclear magnetic resonance studies

Fig. 5 shows a plot of chemical shift as a function of pH where (a), (b) and (c) refer to the chemical shifts of the methylene protons adjacent to the carbonyl, amine and amide groups (in Fig. 1), respectively. There is no significant change in the chemical shift of the (a) protons while (b) and (c) shift substantially. This is a clear indication that the terminal amines are undergoing deprotonation. Since the molecule is symmetrical and the protons undergo rapid chemical exchange, only a single set of resonances is seen. The inflection point in the chemical shift curve can be used to estimate the average pK_a of the two protonation sites. The value of 9.5 is in very good agreement with the average value of 9.52 obtained potentiometrically.

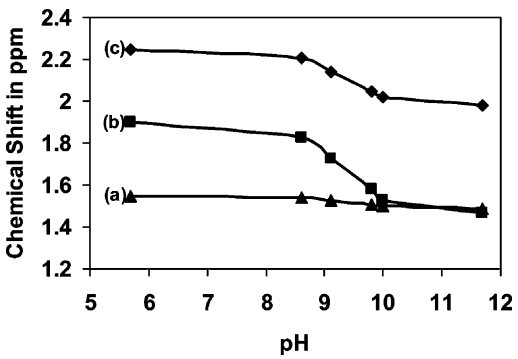

Fig. 5 Change in proton chemical shift (ppm) as a function of pH of 0.015 mol dm^{-3} cageL at 25 °C. The protons are labeled according to Fig. 1.

Fig. 6 shows the effect of Cu(II) on the spectrum of cageL. Cu(II) is paramagnetic which can affect both the chemical shift and relaxation time of the protons. This manifests itself in a broadening and shifting of the NMR signals. The broadening effect of the metal is attenuated by $1/r^6$ where r is the internuclear distance between the Cu(II) and the observed proton. Copper(II) exchange is very rapid and so only an average spectrum is seen. Inspection of Fig. 6 shows that at pH 4 no complexation has taken place as none of the signals are broadened. At pH 6.2, the (b) proton signal has

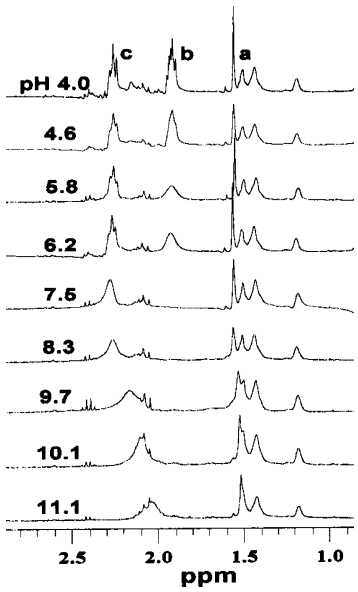

Fig. 6 Proton NMR spectra for complexation of Cu(II) (0.007 M) with cageL (0.015 M) as a function of pH. The protons are labeled according to Fig. 1.

broadened substantially and by pH 7.5 has virtually disappeared into the baseline. This is a clear indication that complexation starts at the terminal amine. The fact that the (c) proton signals do not broaden at the same rate indicates that they are not at the same distance from the metal ion. If the amide was also coordinated one would expect signals (b) and (c) to broaden at the same rate. Above pH 8.3 the (c) protons do broaden while the (a) protons are still relatively sharp. This is consistent with coordination switching from the carbonyl group to the amide nitrogen. These results support the structures postulated above for the different species.

Molecular mechanics

Molecular mechanics has been used extensively to study the preferred conformation of organic molecules. However, its use in inorganic chemistry or coordination chemistry is not as extensive. The main reason for this is the difficulty of obtaining a reliable force field which will accurately describe the bonding of metals. A second problem is the large number of different coordination geometries available to metal ions. Notwithstanding these difficulties, Accelrys have developed the extensible systematic force field (esff).[49] This force field employs semi-empirical rules to translate atomic-based parameters to parameters typically associated with a covalent force field. The force field has been applied to molecular simulations of a wide variety of systems including transition metal complexes.[50]

Fig. 4 shows the optimised structures for the different possible isomers of Cu(II)–cageL. It is not possible to compare the total potential energy because of the different bonding and overall charge of the different structures. However, the internal energy represents the strain energy introduced into the ligand when it is forced to adopt a particular conformation upon metal binding. It is, therefore, one of the components of the total potential energy, the others being the ligand field stabilization energy, electrostatic interaction energy and van der Waal's energy. Care must be exercised in comparing these energies to the measured

Table 3 Bonding potential energies differences (kcal mol^{-1}) calculated for ligand conformations found in the four possible structures of MLH_{-1} (Fig. 4) relative to the ligand in its lowest energy conformation (cvff force field) together with the total internal potential energy of the metal complex (esff force field)[49]

	Structures			
Energy	e	f	g	h
Total	21.5	46.9	30.1	42.2
Bond	−2.3	5.8	−2.2	−3.3
Angle	8.4	18.0	5.5	11.0
Torsion	14.8	20.1	26.0	34.3
Total for complex	107.8	109.8	102.2	102.4

thermodynamic equilibrium constants because no account has been taken of possible entropy changes. Notwithstanding these limitations, the internal potential energy can be useful in assessing the viability of a proposed structure.

Since it is difficult to compare the potential energy of complexes with differing modes of coordination, we have calculated the change in internal potential energy of the ligand in going from its lowest energy conformation to the conformation depicted in the optimised structures given in Fig. 4. Thus this change in potential energy represents the ligand conformational penalty which must be paid in order for the ligand to coordinate to the metal ion. The internal potential energy of the lowest energy conformation of the ligand is 102.4 kcal mol^{-1}. This high potential energy comes mainly from the strain within the cage structure, in particular the angle bending and torsion angle energies. By forcing the ligand to adopt a particular conformation so that it can coordinate to the metal ion, the internal potential energy increases. Table 3 lists the potential energy increase of 4 possible structures for the MLH_{-1} complex. In the previous section, it was argued that structure 4(e) was unlikely because of the large chelate ring. This structure has the highest internal strain energy. Also, a change in coordination from amide carbonyl to amide nitrogen 4(f) to 4(g) increases the torsion angle strain by 12 kcal mol^{-1}. Most of this strain energy comes from distortion of the amide bond planarity as shown in Fig. 4. The most likely structure was postulated to be 4(h). This structure has the 2nd highest strain energy which comes from bond angle and torsion angle distortion. However, in this structure the ligand is also quadradentate, while in the other 3 isomers it is tridentate. In order to form then, the bond strength of the metal amine bond must more than compensate for the increase in strain energy. Using the esff force field it is possible to calculate the internal energy of the complex. When the metal is included in the calculation then structure 4(h) does indeed have the lowest internal energy.

Blood plasma simulation

The design of copper based anti-inflammatory drugs is based, amongst other things, upon the ability of the ligand to mobilize copper *in vivo* as reflected by a high plasma mobilizing index (p.m.i.). P.m.i. of a ligand for a metal ion is defined as the percentage increase in the total concentration of low molecular mass complexes of the metal ion caused by the ligand. The calculation of p.m.i. takes into account competition between the ligand and all the endogenous metal ions and low molecular mass ligands present in blood plasma. In calculating the p.m.i curves use has been made of the ECCLES model[51] of blood plasma to which the constants determined in this study have been added. Fig. 7(a) gives the p.m.i. curves for cageL and some related ligands. These curves show that cageL mobilizes Cu(II) more than L^1, however, it is much poorer than L^6. The reason for this is the relatively high affinity of cageL for Zn(II) and Ca(II). Fig. 7(b) shows that cageL causes substantial mobilization of Ca(II) and Zn(II) and so there is little of the ligand left to complex Cu(II). These results indicate that cageL could find application as a carrier of copper in dermal absorption but that it would release any bound copper once it entered the circulatory system.

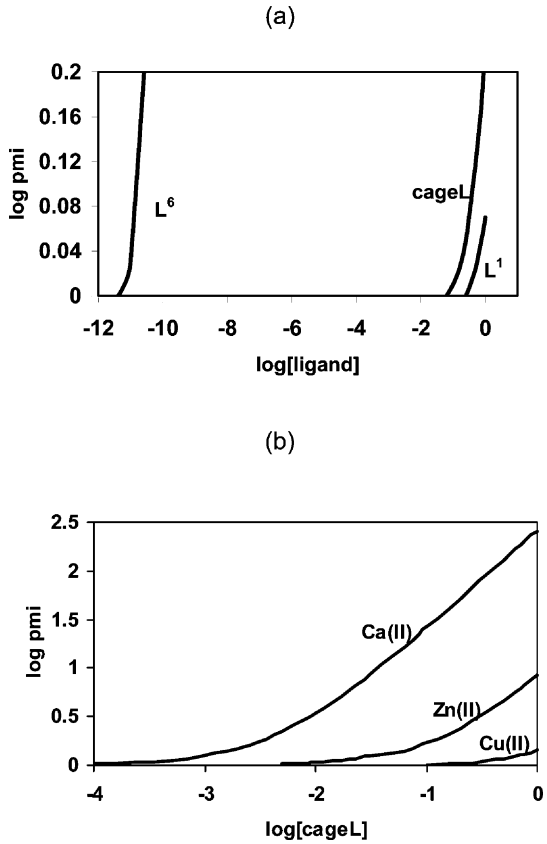

Fig. 7 P.m.i. curves for (a) Cu(II) with L^1, L^6 and cageL, and (b) cageL with Cu(II), Zn(II) and Ca(II).

Superoxide dismutase mimetic activity studies

The beneficial role of copper in minimizing inflammation has been attributed to its redox activity, particularly the ability of copper in such enzymes as superoxide dismutase (SOD) to remove the highly pro-inflammatory superoxide anion radical.[52,53] Along with hydrogen peroxide and hydroxyl radical, superoxide has been implicated in oxidative damage phenomena related to aging, inflammation and post-ischaemic injury *via* reperfusion.[53,54] Copper-zinc superoxide (CuZn-SOD) is an enzyme that catalyses the dismutation of the superoxide anion radical to molecular oxygen, water and/or hydrogen peroxide. A number of copper(II) complexes including those of polypeptides have been reported to exhibit SOD-mimic activity and thus are viewed as alternative human therapeutics to remove pro-inflammatory superoxide anion radical *in vivo*.[52,55] We investigated the SOD activity of the

[Cu(II)-cageLH$_{-1}$] complex using the NBT assay[52,56,57] by measuring the concentration of the complex required to reduce diformazan formation by 50% (also termed as the IC_{50} value). An IC_{50} value of 233 μmol dm^{-3} for the [Cu(II)-cageLH$_{-1}$] species was determined. This value is much higher than the IC_{50} of 0.011 μmol dm^{-3} for the native CuZn-SOD.[58] The high IC_{50} value exhibited by the [Cu(II)-cageLH$_{-1}$] complex is indicative of its very low SOD mimetic activity. This may be due to the unavailability of the binding sites for the superoxide anion radical to coordinate to the metal ion.

IC_{50} values of Cu(II) complexes of amino acids such as tyrosine (45 μmol dm^{-3}) and lysine (86 μmol dm^{-3}) and, non-steroidal anti-inflammatory drugs (NSAIDs) such as salicylates (2–28 μmol dm^{-3}) have been reported.[59,60] These values are also lower than that obtained in this study. However, we have previously reported IC_{50} values of 58 and 110 μmol dm^{-3} for related ligands.[12,13]

1-octanol–water partition coefficient studies

One important aspect upon which biological activity depends is the ability of the drug to reach the target area. For dermal absorption transport across the skin and bio-membranes in general is a process of limited diffusion governed by the drug's chemical and physical properties such as lipophilicity and protein binding.[61,62] For this reason, this study also investigated the octanol/water partition coefficients of copper complexes with a view of establishing whether these species can be administered transdermally. The octanol/water mixture was used as a bio-phase model of the membrane.

Fig. 8 shows the logarithm of the partition coefficients (log $P_{oct/aq}$) of Cu(II)–cageL complexes plotted as a function of pH. Observed in Fig. 8 is the fact the all log $P_{oct/aq}$ values are negative, thus indicating that these complexes are largely hydrophilic. The low log $P_{oct/aq}$ values in the acidic pH range 3–4 are due to the high concentration of hydrated $[Cu(OH_2)_6]^{2+}$ in this region. Complexation of Cu(II) with cageL begins at pH 2.5 with formation of MLH species predominating at pH 5.1 thus giving a log $P_{oct/aq}$ value of −2.44. A log $P_{oct/aq}$ value of −1.82 is assigned to the ML species on the basis of the distribution curves (Fig. 3) for the Cu(II)–cageL system. The log $P_{oct/aq}$ at the physiological pH 7.4 is −1.65, can be approximated as the value for MLH$_{-1}$ species. Positive log $P_{oct/aq}$ values in the range 0.618 to 4.128 of some anti-inflammatory drugs have been reported.[63] This suggests that for a drug (complex) to be reasonably lipophilic, the log $P_{oct/aq}$ value must be at least 0.618. However, several workers[64–66] studied ^{64}Cu-labeled complexes of log $P_{oct/aq}$ values in the range −1.60 to −3.02 and therefore, our results fall within this region.

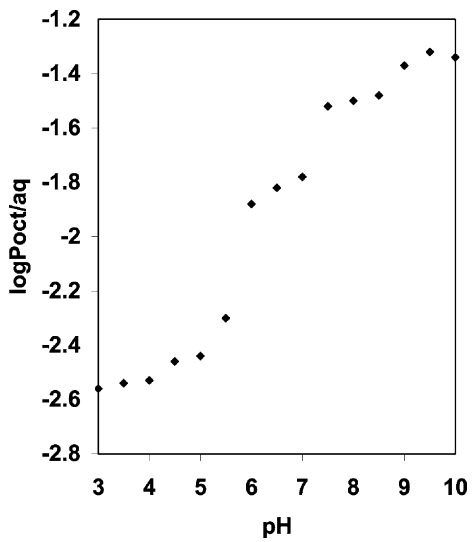

Fig. 8 Cu(II)–cageL partition coefficients measured at 25 °C and an ionic strength of 0.15 mol dm^{-3} (Cl$^-$) as a function of pH.

Although the results for the partition coefficient studies suggest that the copper(II) complexes of cageL are largely hydrophilic, at least 2.9% of the Cu(II)–cageL complexes is extracted into the organic phase of the octanol–water mixture at physiological pH. The contributing factors to the hydrophilicity of these complexes may be the presence of coordinated water molecules, hydrogen bonding and the overall charge of the MLH, ML and MLH$_{-1}$ complexes.

Bio-distribution experiments on mice

Based on the aforementioned *in vitro* results, it was deemed necessary to perform bio-distribution experiments. Since the body is a dynamic system, the bio-distribution was measured as a function of time. Table 4 shows the bio-distribution of ^{64}Cu-labelled Cu(II)–cageL and $CuCl_2$ at 6 and 24 h post-injection. The results revealed an initial rapid clearance of [^{64}Cu]Cu(II)–cageL complex from the blood and rapid uptake by the liver. The high uptake by the liver is due to the fact that copper storage and metabolism occurs in this organ. The Cu(II)–cageL complex has a much longer biological half-life than the copper complexes of L[1], L[6] and L[7]. The [^{64}Cu]$CuCl_2$ used as a control, was rapidly excreted *via* hepatobiliary and renal routes. The activity retention in the body for the [^{64}Cu]Cu(II)-cageL system is about 50% dose as compared to 20% dose for the control. Such activity accumulation and retention over 24 h in the body is encouraging and merits evaluation of this copper chelating agent for possible use in

Table 4 % Dose per organ and per gram tissue (in brackets) for bio-distribution of [^{64}Cu]Cu(II)–cageL species (mean ± std. dev., $n = 3$)

	[^{64}Cu]Cu(II)–cageL		[^{64}Cu]$CuCl_2$	
Organ	6 h	24 h	6 h	24 h
Blood	1.07 ± 0.17 (0.87 ± 0.10)	1.86 ± 0.14 (1.49 ± 0.25)	0.80 ± 0.23 (0.62 ± 0.17)	0.86 ± 0.24 (0.71 ± 0.22)
Carcass	6.94 ± 0.79 (0.61 ± 0.05)	13.25 ± 2.87 (1.16 ± 0.35)	7.85 ± 1.87 (0.63 ± 0.17)	11.35 ± 1.77 (0.95 ± 0.20)
Head	2.00 ± 0.26 (0.63 ± 0.08)	3.72 ± 0.21 (1.13 ± 0.17)	1.94 ± 0.04 (0.59 ± 0.02)	7.56 ± 2.74 (2.60 ± 1.09)
Heart	0.28 ± 0.04 (1.78 ± 0.19)	0.44 ± 0.04 (3.55 ± 0.38)	0.19 ± 0.02 (1.56 ± 0.15)	0.21 ± 0.07 (1.73 ± 0.43)
Intestines	16.80 ± 4.97 (5.84 ± 2.00)	25.34 ± 5.61 (9.09 ± 4.09)	22.17 ± 2.87 (8.14 ± 1.12)	11.61 ± 6.94 (3.95 ± 1.86)
Kidney	1.15 ± 0.09 (3.18 ± 0.17)	1.94 ± 0.01 (5.10 ± 0.20)	1.04 ± 0.15 (3.09 ± 0.41)	0.96 ± 0.42 (3.03 ± 1.03)
Liver	67.89 ± 5.42 (56.36 ± 1.65)	33.57 ± 7.56 (30.69 ± 7.56)	63.69 ± 5.06 (56.20 ± 0.45)	11.39 ± 7.11 (11.32 ± 0.64)
Lung	0.61 ± 0.07 (3.33 ± 0.41)	0.96 ± 0.04 (5.74 ± 0.81)	0.53 ± 0.08 (1.85 ± 0.25)	0.44 ± 0.18 (2.27 ± 0.34)
Muscle	0.07 ± 0.01 (0.44 ± 0.10)	0.15 ± 0.09 (0.90 ± 0.18)	0.06 ± 0.04 (0.42 ± 0.13)	0.04 ± 0.03 (0.25 ± 0.10)
Spleen	0.28 ± 0.05 (2.30 ± 0.13)	0.44 ± 0.11 (3.86 ± 0.38)	0.23 ± 0.04 (1.73 ± 0.13)	0.12 ± 0.02 (1.32 ± 0.11)
Urine	2.89 ± 1.08	18.34 ± 2.52	1.50 ± 1.29	55.44 ± 8.72

Table 5 % Dose per organ and per gram tissue for the bio-distribution of the dermally absorbed [^{64}Cu]Cu(II)–cageL complexes (mean ± std. dev., $n = 4$) 24 h post-dosing

	[^{64}Cu]Cu(II)-cageL		[^{64}Cu]$CuCl_2$	
Organ	Per organ	Per gram	Per organ	Per gram
Blood	0.21 ± 0.03	0.19 ± 0.05	2.25 ± 0.08	1.50 ± 0.23
Carcass	10.50 ± 2.88	0.96 ± 0.27	14.20 ± 10.2	0.89 ± 0.59
Head	8.63 ± 2.66	3.08 ± 0.91	3.34 ± 0.67	1.02 ± 0.20
Heart	0.04 ± 0.02	0.48 ± 0.26	0.37 ± 0.07	2.10 ± 0.43
Intestines	10.83 ± 6.80	4.00 ± 2.59	20.92 ± 2.53	6.27 ± 0.70
Kidney	0.22 ± 0.17	0.85 ± 0.60	1.74 ± 0.27	3.61 ± 0.63
Liver	1.57 ± 1.00	1.52 ± 1.05	18.48 ± 3.16	13.80 ± 2.52
Lung	0.08 ± 0.06	0.81 ± 0.50	0.67 ± 0.12	3.04 ± 0.52
Muscle	0.04 ± 0.02	0.52 ± 0.53	0.13 ± 0.03	0.58 ± 0.27
Spleen	0.06 ± 0.03	0.79 ± 0.42	0.19 ± 0.02	2.11 ± 0.35
Urine	67.82 ± 9.39		37.80 ± 13.4	

chemotherapy and diagnosis. However, this complex is unlikely to penetrate the blood–brain barrier in view of its octanol–water partition coefficient.

Anderson *et al.*[67,68] have investigated thermodynamically and kinetically stable ^{64}Cu-labelled macrocyclic complexes with different formal charges as biofunctional chelators. All the complexes were observed to be rapidly cleared from circulation and positively charged complexes had higher uptake and slow clearance. Other reporters[63–65] have shown that positively charged ^{64}Cu complexes of the macrocyclic ligands exhibited rapid uptake in the liver and kidneys with slow clearance, whereas the negatively charged and neutral complexes cleared rapidly from all tissues by the renal route.

Since the preferred route of administration is as a cream *via* the skin, bio-distribution studies were also performed using dermal absorption. Results of cageL and $CuCl_2$ control are given in Table 5. Of note here is that the same bio-distribution as intravenous injection is not obtained. With dermal absorption less activity is excreted in the urine and more activity is retained in the body.

Conclusions

In this study we have shown that incorporation of the pentacycloundecane cage derivative into a diaminodiamide ligand does not affect the ability of the ligand to complex copper(II). Indeed, the rigidity of the cage appears to increase the stability of the complexes. This is presumably because the ligand is pre-formed in the correct conformation for metal binding. The bio-distribution and dermal absorption studies show that Cu(II) complexes of cageL survive *in vivo.*

Experimental

Synthesis of the novel oxahexacyclododecane diester 6

To a suspension of the diacid **4** (0.552 g, 2.00×10^{-3} mol) in dry dichloromethane (10 ml) was added oxalyl chloride (2 ml, 2.30×10^{-2} mol) drop-wise with stirring under nitrogen. The solution was stirred for a further 5 h after the reaction became homogeneous and concentrated under *vacuo* to yield the diacyl choride **5** as a colourless oil. Excess ethanol ~50 ml was then added to the diacyl chloride and the mixture was stirred under nitrogen for 18 h. The reaction mixture was concentrated *in vacuo*, dissolved in deionised water and extracted with ethyl acetate. The organic extract was concentrated *in vacuo* to yield the diester (0.550 g) as a light yellow oil. ^{1}H NMR [$CDCl_3$, 400 MHz]: δ_H 2.72 (m, 2H), 2.61 (m, 2H), 2.38 (m, 2H), 1.47 (d, H_{4a}, J 10.44 Hz), 1.83 (d, H_{4s}, J 10.44 Hz), 2.64 (m, 2H), 2.79 (s, 2H), 4.10 (q, 2H, H_{16}, H_{21}, J 7.142), 1.22 (t, 2H); ^{13}C NMR [$CDCl_3$, 100 MHz]: δ_c 48.4 (d), 41.8 (d), 44.5 (d), 43.3 (t), 92.8 (s), 59.1 (d), 92.8 (s), 38.4 (t), 170.4 (s), 60.4 (t), 14.1 (q), and elemental analysis calculated for $C_{19}H_{24}O_5$: C, 68.66; H, 7.28%: found C, 68.76, H, 7.31%.

Synthesis of 3,5-diaminodiamido-4-oxahexacyclo[5.4.1.0^{2,6}.0^{3,10}.0^{5,9}.0^{8,11}]dodecane 7

Freshly distilled ethylenediamine (~50 ml) was added to the diester **6** (0.500 g, 1.50×10^{-3} mol) and the reaction mixture was refluxed for 20 h under nitrogen. The excess ethylenediamine was removed *in vacuo.* The product **7** was extracted with tetrahydrofuran and concentrated *in vacuo* to give a light brown oil (0.500 g, 92%). ^{1}H NMR [$CDCl_3$, 400 MHz]: δ_H 2.53 (m, 2H), 2.56 (m, 2H), 2.33 (m), 1.40 (d, H_{4a}, J 10.44 Hz), 1.75 (d, H_{4s}, J 10.44 Hz), 2.50 (m, 2H,), 2.58 (s, 2H), 7.19 (2H), 3.13 (t, 2H), 2.64 (t, 2H), 1.90 (2H), ^{13}C NMR [$CDCl_3$, 100 MHz]: δ_c 47.9 (d), 41.2 (d), 43.9 (d), 43.2 (t), 93.6 (s), 58.4 (d), 39.3 (t), 170.05 (s), 41.64 (t), 40.95 (t), and elemental analysis calculated for $C_{19}H_{28}N_4O_3$: C, 63.33; H, 7.77, N, 15.55%: found C, 63.76, H, 7.77, N, 15.96%. The NMR spectra were recorded on a Varian Unity Inova 400 MHz spectrometer. Elemental analyses were obtained from a Leco CHNS 932 instrument. The purity of cageL was confirmed by acid–base titration and was found to be greater than 95%.

Potentiometric measurements

All solutions for potentiometry were prepared in glass distilled water which had been boiled to remove dissolved carbon dioxide. Recrystallized NaCl was used as background electrolyte at an ionic strength of 0.15 mol dm^{-3} (Cl^-). Other reagents, copper(II) chloride dihydrate, zinc(II) chloride dihydrate, HCl, NaOH and EDTA (Merck) were commercially available and of analytical grade. These were used without purification. The 0.1 mol dm^{-3} solutions of NaOH and HCl were prepared from Merck Titrisol ampoules and standardized by titrating with potassium hydrogen phthalate (KHP) and sodium tetraborate decahydrate (Borax), respectively, using standard methods of Vogel. The NaOH solutions prepared were further standardized against standard HCl solution. Potentiometric data were collected, under an inert atmosphere of purified nitrogen, at 25 °C, using an automatic titration procedure described previously.[10,12] The data were analysed using the ESTA suite of computer programs.[39] The slope of the glass electrode (Metrohm 6.0222.100) was determined from a buffer line and the final $E°$ determined *in situ.* Carbonate contamination of the titrant solutions was checked by titration using the Gran method.[69] Under these conditions the water ionization constant was determined to be 13.73 log units.

UV-visible and nuclear magnetic resonance spectroscopy

UV-visible spectra were recorded at 25 °C on a Hewlett Packard 8425A Diode Array in the wavelength region between 340 and 800 nm. Aqueous solutions containing 1 : 2 ratio Cu(II) : cageL were taken over pH range 2–11. Small amounts of 0.1 mol dm^{-3}

NaOH and HCl were used to adjust the pH during the titration. NMR samples, 0.015 mol dm^{-3} of cageL solution and a solution of 1 : 2 molar ratio of the Cu(II) to cageL were prepared in D_2O. ^1H NMR spectra were recorded on a Varian Unity Plus 400 MHz instrument. The pH of the solutions was adjusted using NaOD or DCl. The pH values were not corrected for the isotope effect.

Molecular mechanics

Molecular mechanics calculations were performed using the Discover 3 module of the Accelrys life sciences molecular modelling software, InsightII.[49] For the free ligand, the cvff force field was used while for the metal complex the esff force field was used.

Blood plasma simulation, superoxide dismutase mimic activity and octanol–water partition coefficient studies

Blood plasma modelling was carried out by incorporation of the formation constants determined in this study into a blood plasma model[70,71] consisting of data for 10 metal ions and more than 5000 ligands. This enlarged database was efficiently and conveniently interrogated by the Evaluation of Constituent Concentrations in Large Equilibrium Systems (ECCLES) computer program to yield results pertaining to the influence of the chelating agents on the equilibria in terms of the plasma mobilizing index (p.m.i) of each agent. P.m.i, defined as the ability to move metal from a protein bound form to a low-molecular weight form, can be represented by the following expression;

$$\text{p.m.i} = \frac{(\text{total concentration of low-molecular-weight metal complex species in the presence of drug})}{(\text{total concentration of low-molecular-weight metal complex species in normal plasma})}$$

SOD mimetic activity of the Cu(II)–cageL system was determined using nitroblue tetrazolium (NBT) assay as described earlier.[12] Partition coefficients were measured at 25 °C and an ionic strength of 0.15 mol dm^{-3} (Cl^-) using the shake flask method reported previously.[12]

Bio-distribution and dermal absorption studies

^{64}Cu was prepared by neutron irradiation of 1.7–2.5 mg copper(II) oxide (99.9999%, Aldrich Chem. Co., WI, USA) for 24 h at a thermal neutron flux of 1.0×10^{14} neutrons cm^{-2} s^{-1} in Safari-1 Research Reactor. The targets were dissolved in 1.0 ml 1.0M HCl and diluted to 3.0 ml with 1.0 M HCl. Typical specific activities of ~600 MBq mg^{-1} target material were obtained.

^{64}Cu-labelled Cu(II)–cageL complex was prepared by spiking 20 cm^3 of Cu^{2+} (0.001 mol dm^{-3})–cageL (0.003 mol dm^{-3}) solution with 10 mCi $^{64}CuCl_2$(aq) (Radiochemical purity >98%). Bio-distribution studies were carried out by injecting 6–8 weeks old Balb/c mice with 0.2 cm^3 of 5 μCi [^{64}Cu]Cu(II)–cageL solution and $^{64}CuCl_2$(aq) in control experiments. At 6 and 24 h post-injection time points, groups of mice (three at a time) were anaesthetized by carbon monoxide inhalation and aliquots of blood were taken from the heart. Various samples were removed, rinsed with NaCl (0.9%), dried and then weighed. The radioactivity in these samples as well as in 10 cm^3 aliquots of urine extract were counted using a Minaxi Auto-gamma 5000 Series counter with the window set at 340–540 KeV. The dermal absorption experiments were performed by applying 0.2 cm^3 of 5 μCi [^{64}Cu]Cu(II)–cageL and $^{64}CuCl_2$(aq) dosing solutions on the enclosed skin of the anterior dorsal side of the test animals. The application site was prepared by clipping an area of approximately 2 × 2 cm on the dorsal side of all test animals 15 h prior to dosing. The animals were anaesthetized with saline solution of ketamine/xylazine following clipping and a small tubing ring (1.2 cm diameter and 0.5 cm height) was fixed to their backs using cyanoacrylate adhesive. At 24 h post-dosing time point, groups of mice (four at a time) were anaesthetized by carbon monoxide inhalation and the procedure for removing samples followed that of bio-distribution experiments. The percentages of radio-activity dose per organ and/or per gram (g) tissue were computed from the mean organ weights after correction for radio-activity decay.

The bio-distribution and dermal absorption studies on mice were approved by the Research Animals Ethics Committee of the University of Cape Town (permission number 005/039). The authority to possess and use radioactive nuclide ^{64}Cu was granted by the university's radiation protection and health safety committee in conjunction with the Department of Health (authority number 33/01/0327).

Caution: ^{64}Cu decays by positrons emissions, which annihilate to produce tissue penetrating high energy γ-radiation. Therefore, it is advisable to use much less activity of ^{64}Cu and perform all experiments behind lead bricks inside a fume cupboard.

Acknowledgements

The authors thank the Botswana Government and the Councils of the Universities of Cape Town and KwaZulu-Natal for financial support and a scholarship to S. O. We are also grateful to Dr J. R. Zeevaart and D. Jansen (South African Nuclear Energy Cooperation (Ltd) for supplying us with $^{64}CuCl_2$ and, J. Boniaszczuk (Nuclear Medicine Dept), J. Visser (Animal Unit), Dr J. N. Zvimba and T. Jackson for technical assistance with animal experiments.

References

1 D. J. MacCarthy, *Arthritis and Allied Conditions, A textbook of Rheumatology*, 11th edn, Lea and Febiger, Philadelphia, 1989, p. 507.
2 A. Aeschlinmann, B. R. Simmen and B. A. Michel, in; *Rheumatoid Arthritis*, ed. H. Baumgartner, J. Dvorak, D. Grob, U. Munzinger and B. R. Simmen, Thieme Medical Publishers, Inc., New York, 1985.
3 R. F. Wilkens and S. L. Dahl, *Therapeutic Controversies in the Rheumatic Disease*, 1987, Grune and Stratton, Inc., Orlando.
4 J. R. J. Sorenson, *Prog. Med. Chem.*, 1976, **19**, 135.
5 J. R. J. Sorenson, *Prog. Med. Chem.*, 1978, **15**, 211.
6 J. R. J. Sorenson, *Prog. Med. Chem.*, 1989, **26**, 437.
7 J. R. J. Sorenson, in *Metal ions in biological Systems, Inorganic Drugs in Deficiency and Disease*, ed. H. Sigel, Marcel Decker, Inc., 1982, vol. 14, p. 77.
8 G. E. Jackson and M. J. Kelly, *J. Chem. Soc., Dalton Trans.*, 1989, 2429.
9 G. E. Jackson, P. W. Linder and A. Voye, *J. Chem. Soc., Dalton Trans.*, 1996, 4605.
10 G. E. Jackson, L. Gama-Mkhonta, A. Voye and M. J. Kelly, *J. Inorg. Biochem.*, 2000, **79**, 147.
11 S. Odisitse, *MSc Thesis*, University of Cape Town, 2003.
12 T. E. Nomkoko, G. E. Jackson, B. S. Nakani, K. A. Louw and J. R. Zeevaart, *Dalton Trans.*, 2004, 741.
13 T. E. Nomkoko, G. E. Jackson and B. S. Nakani, *Dalton Trans.*, 2004, 1432.
14 G. E. Jackson, in *Handbook of Metal–Ligand Interactions in Biological Fluids, Bioinorganic Chemistry*, ed. G. Berthon, Marcel Dekker, Inc., New York, 1995, vol. 2, p. 1228.
15 A. P. Marchand, *Chem. Rev.*, 1989, **89**, 1011.
16 G. W. Griffin and A. P. Marchand, *Chem. Rev.*, 1989, **89**, 997.

17 A. P. Marchand, in *Advances in Theoretically Interesting Molecules*, ed. R. P. Thummel, JAI Press, Greenwich, CT, vol. 1, 1989, 357.
18 D. W. Oliver, D. G. Dekker, F. O. Snykers and T. G. Fourie, *J. Med. Chem.*, 1991, **34**, 851.
19 D. W. Oliver, D. G. Dekker and F. O. Snyckers, *Eur. J. Med. Chem.*, 1991, **26**, 375.
20 D. W. Oliver, D. G. Dekker and F. O. Snyckers, *Drug Res.*, 1991, **41**, 545.
21 Y. Inamoto, K. Aiyami, N. Tasaishi and Y. J. Fujikura, *J. Med. Chem.*, 1967, **19**, 536.
22 Y. Inamoto, K. Aiyami, T. Kadono, H. Makayama, A. Takatsuki and G. Tumura, *J. Med. Chem.*, 1977, **20**, 1371.
23 J. C. A. Boeyens, L. M. Cook, G. N. Nelson and T. G. Fourie, *S. Afr. J. Chem.*, 1994, **47**(2), 72.
24 R. S. Schab, A. C. England, D. C. Poskanzer and R. R. Young, *J. Am. Med. Assoc.*, 1969, **208**, 1168.
25 J. L. Neumeyer, in *Principles of Medicinal Chemistry*, ed. W. O. Foye, Lea and Febiger, London, 1989, p. 223.
26 K. Gerzon and D. Kou, *J. Med. Chem.*, 1967, **10**, 189.
27 K. Gerzon, R. J. Kraay and R. T. Rapala, *J. Med. Chem.*, 1965, **8**, 580.
28 A. N. Voldeng, C. A. Bradley, R. D. Kee, E. L. Knight and F. L. Melder, *J. Pharm. Sci.*, 1968, **57**, 1053.
29 K. B. Brookes, P. W. Hickmott, K. K. Jutle and C. A. Schreyer, *S. Afr. J. Chem.*, 1992, **45**, 8.
30 W. J. Geldenhuys, S. F. Malan, J. R. Bloomquist, A. P. Marchand and C. J. Van der Schyf, *Med. Res. Rev.*, 2005, **25**(1), 21.
31 R. C. Cookson, E. Grundwell, R. R. Hill and J. Hudec, *J. Chem. Soc.*, 1964, 3062.
32 A. P. Marchand, Z. Huang, Z. Chen, H. K. Hariprakasha, I. N. N. Namboothiri, J. S. Brodbelt and M. L. Reyzer, *J. Heterocycl. Chem.*, 2001, **38**, 1361.
33 T. Govender, H. K. Hariprakasha, H. G. Kruger and A. P. Marchand, *Tetrahedron: Asymmetry*, 2003, **14**, 1553.
34 A. P. Marchand, K. A. Kumar, A. S. McKim, K. M. Majerski and G. Kragol, *Tetrahedron*, 1997, **10**, 3467.
35 G. A. Boyle, T. Govender, H. G. Kruger and G. E. M. Maguire, *Tetrahedron: Asymmetry*, 2004, **5**(17), 2661.
36 T. Govender, H. K. Hariprakasha, H. G. Kruger and A. P. Marchand, *Tetrahedron: Asymmetry*, 2003, **14**(11), 1553.
37 J. C. Rossotti and H. Rossotti, *J. Chem. Educ.*, 1965, **42**, 375.
38 G. E. Jackson and M. J. Kelly, *J. Chem. Soc., Dalton Trans.*, 1989, 2429.
39 K. Murray and P. M. May, *ESTA (Equilibrium Simulation for Titration Analysis) manual, Version. 3*, UWIST, Cardiff, Wales, 1989.
40 D. R. Williams, *The metals of Life*, van Nonstrand Reinhold Company, London, 1971.
41 H. H. Jaffe and M. Orchin, *Theory and Application of Ultraviolet Spectroscopy*, John Wiley & Sons, New York, 1962.
42 A. E. Martel, R. M. Smith and R. J. Motekaitis, *NIST Critical Stability Constants of Metal Complexes Database*, Texas A&M University College Station, TX, 1993.
43 E. J. Billo, *Inorg. Nucl. Chem. Lett.*, 1974, **10**, 613.
44 H. Sigel and A. E. Martell, *Chem. Rev.*, 1982, **82**, 385.
45 F. J. Quaeyhaegens, H. O. Desseyn, S. P. Perlepes, J. C. Plakatouras, B. Bracke and A. T. H. Lenstra, *Transition Met. Chem.*, 1991, **16**, 92.
46 A. Zuberbuhler and Th. Kaden, *Helv. Chim. Acta*, 1968, **51**, 1805.
47 H. Ojima and K. Nonoyama, *Coord. Chem. Rev.*, 1988, **921**, 857.
48 R. M. Lewis, G. H. Nancollas and P. Coppens, *Inorg. Chem.*, 1972, **11**, 1371.
49 InsightII, System Guide, issued by Accelrys, Cambridge, UK, July 2005.
50 S. Shia, L. Yan, Y. Yang, J. Fisher-Shaulsky and T. Thacher, *J. Comput. Chem.*, 2003, **24**(9), 1059.
51 G. E. Jackson, P. M. May and D. R. Williams, *J. Inorg. Nucl. Chem.*, 1978, **40**, 1227.
52 M. Gonzalez-Alvarez, G. Alzuet, J. Borras, L. C. Agudo and J. M. Montego-Bernado, *J. Biol. Inorg. Chem.*, 2003, **8**, 112.
53 I. Fridovich, *J. Biol. Chem.*, 1989, **264**(14), 7761.
54 V. Pelmenschikov and P. E. M. Siegbahn, *Inorg. Chem.*, 2005, **44**(9), 3311.
55 R. N. Patel and K. B. Pandega, *J. Inorg. Biochem.*, 1998, **72**, 109.
56 C. Auclair and E. Voisin, in *CRC Handbook of Methods for Oxygen Radical research*, ed. R. A. Greenwald, 1985, CRC Press, Boca Raton, FL.
57 I. Fridovich, in *CRC Handbook of Methods for Oxygen Radical research*, ed. R. A. Greenwald, 1985, CRC Press, Boca Raton, FL.
58 H.-L. Zhu, L.-M. Zheng, D.-G. Fu, X.-Y. Huang, M.-F. Wu and W.-X. Tang, *J. Inorg. Biochem.*, 1998, **70**, 211.
59 C. T. Dillion, T. W. Hambley, B. J. Kennedy, P. A. Lay, Q. Zhou, N. M. Davies, J. R. Biffin and H. L. Regtop, *Chem. Res. Toxicol.*, 2003, **16**, 28.
60 J. E. Weder, C. T. Dillion, T. W. Hambley, B. J. Kennedy, P. A. Lay, Q. Zhou, N. M. Davies, J. R. Biffin, H. L. Regtop and N. M. Davies, *Coord. Chem. Rev.*, 2002, **232**, 95.
61 S. K. Poole and C. F. Poole, *J. Chromatogr., B*, 2003, **797**, 3.
62 G. Klopman and H. Zhu, *Mini-Rev. Med. Chem.*, 2005, **5**, 127.
63 F. Pehourcq, M. Matoga, C. Jarry and B. Bannwarth, *J. Liq. Chromatogr. Relat. Technol.*, 2001, **24**(14), 2177.
64 X. Sun, M. Wuest, Z. Kovacs, A. D. Sherry, R. Motekaitis, Z. Wang, A. E. Martell, M. J. Welch and C. J. Anderson, *J. Biol. Inorg. Chem.*, 2003, **8**, 217.
65 X. Sun, M. Wuest, G. R. Weisman, E. H. Wong, D. P. Reed, C. A. Boswell, R. J. Motekaitis, A. E. Martell, M. J. Welch and C. J. Anderson, *J. Med. Chem.*, 2002, **45**, 469.
66 A. B. Packard, J. F. Kronauge, P. J. Day and S. T. Treves, *Nucl. Med. Biol.*, 1998, **25**, 531.
67 T. M. Jones-Wilson, K. A. Deal, C. J. Anderson, D. W. McCarthy, Z. Kovac, R. J. Motekaitis, A. D. Sherry, A. E. Martell and M. J. Welch, *Nucl. Med. Biol.*, 1998, **25**, 523.
68 C. S. Cutler, M. Wuest, C. J. Anderson, D. E. Reichert, Y. Sun, A. E. Martell and M. J. Welch, *Nucl. Med. Biol.*, 2000, **27**, 375.
69 G. Gran, *Analyst*, 1952, **77**, 309.
70 P. M. May, P. W. Linder and D. R. Williams, *J. Chem. Soc., Dalton Trans.*, 1977, 548.
71 G. E. Jackson and M. J. Kelly, *Inorg. Chim. Acta*, 1988, **152**, 215–217.